IEEE Photonics Journal
An IEEE Photonics Society Publication

Open Access

Efficient Coupling Between Photonic and Dielectric-Loaded Surface Plasmon Polariton Waveguides With the Same Core Material

Volume 6, Number 3, June 2014

Hyun-Jun Lim
Min-Suk Kwon

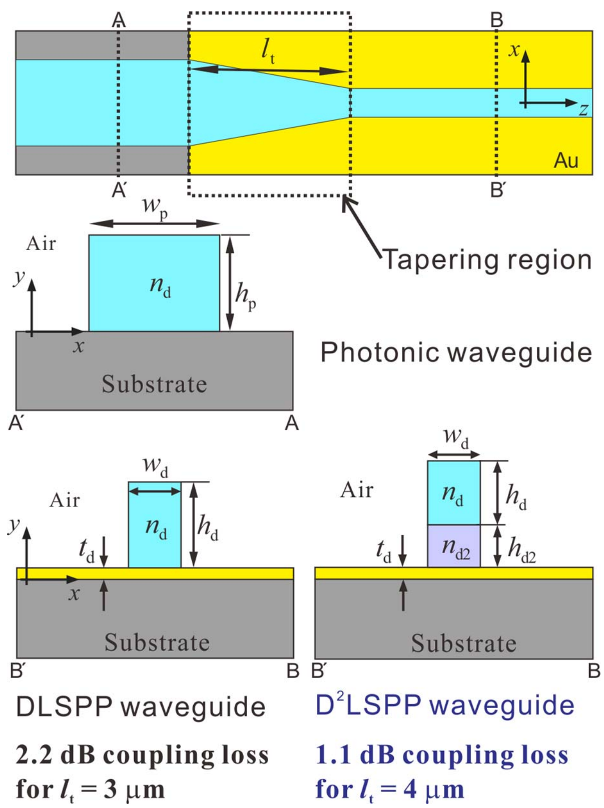

DOI: 10.1109/JPHOT.2014.2326657
1943-0655 © 2014 IEEE

Efficient Coupling Between Photonic and Dielectric-Loaded Surface Plasmon Polariton Waveguides With the Same Core Material

Hyun-Jun Lim and Min-Suk Kwon

School of Electrical and Computer Engineering, Ulsan National Institute of Science and Technology (UNIST), Ulsan 689-798, Korea

DOI: 10.1109/JPHOT.2014.2326657

Manuscript received April 24, 2014; revised May 13, 2014; accepted May 14, 2014. Date of publication May 23, 2014; date of current version June 2, 2014. This work was supported by the Basic Science Research Program through the National Research Foundation of Korea (NRF) funded by the Ministry of Education under Grant 2013R1A1A2A10062227. Corresponding author: M.-S. Kwon (e-mail: mskwon@unist.ac.kr).

Abstract: We theoretically investigate how to efficiently couple a photonic waveguide to a dielectric-loaded surface plasmon polariton (DLSPP) waveguide when they are based on a common core material. The DLSPP waveguide is tapered and butt coupled to the photonic waveguide. First, we propose the use of a dielectric with a higher refractive index than the dielectrics of previous DLSPP waveguides. The photonic and DLSPP waveguides are designed to reduce the loss and tapering region length of the coupling, and the tapering region is optimized. We achieve the coupling between the photonic and DLSPP waveguides based on a dielectric of refractive index of 1.57 with a coupling loss of 2.3 dB through a 3-μm-long coupling region. The coupling loss is further reduced by modifying the DLSPP waveguide into a double-DLSPP (D^2LSPP) waveguide. The D^2LSPP waveguide has an additional low-index dielectric between its high-index dielectric and metal layer. Designed appropriately, the D^2LSPP waveguide can be coupled to the photonic waveguide with a coupling loss of 1.1 dB through a 4-μm-long coupling region. Since the photonic and DLSPP or D^2LSPP waveguides investigated in this paper can be simultaneously fabricated, they may constitute an easily realizable hybrid planar lightwave circuit with a relatively low loss.

Index Terms: Plasmonics, subwavelength structure, waveguide devices.

1. Introduction

Surface plasmon polaritons (SPPs) are electromagnetic waves which travel along metal-dielectric interfaces [1]. Since an SPP is coupled to the collective oscillation of free electrons in a metal surface, its wavelength can be made much shorter than the free-space wavelength λ. Because of this property of SPPs, SPP-based nanoplasmonic waveguides are believed to overcome the diffraction limit: they can support a mode which has a mode area much smaller than $(\lambda/2)^2$ [2]. The strong light confinement of nanoplasmonic waveguides enables a nanoplasmonic waveguide device to efficiently control a light signal in a compact region. Thus a variety of nanoplasmonic waveguides have been investigated. A few examples are metal-insulator-metal (MIM) waveguides [3]–[5], metal-insulator-silicon-insulator-metal (MISIM) waveguides [6]–[10], and dielectric-loaded SPP (DLSPP) waveguides [11]–[13]. Compared to MIM or MISIM waveguides, a DLSPP waveguide has a rather large mode area similar to $[\lambda/(2n_d)]^2$, where n_d is the refractive index of its loaded dielectric (or core material). However, it can be much more easily implemented than MIM or MISIM waveguides. In addition, it has smaller propagation loss than MIM or MISIM waveguides. Moreover, it is a good platform for realizing functional nanoplasmonic devices based on various dielectrics such as electrooptic polymer [14] and polymer with gain [15]. Because of these features, DLSPP-waveguide-based directional couplers [16], ring resonators [17], [18], and Mach-Zehnder interferometers [18], [19] have been developed.

Although the propagation loss of a DLSPP waveguide is relatively small, it is still much larger than that of a photonic waveguide. To circumvent this problem, a hybrid structure which consists of photonic and DLSPP waveguides is required. Photonic waveguides are used to transmit light signals, and DLSPP waveguides are used to control light signals [20]–[23]. In such a hybrid structure, it is essential to efficiently couple a DLSPP waveguide to a photonic waveguide. Although other nanoplasmonic waveguides have been coupled to photonic waveguides through various methods like directional coupling [24], [25], end-fire coupling with or without tapering has been used for DLSPP waveguides. In the case of the hybrid structure based on silicon photonic waveguides, end-fire coupling between a silicon photonic waveguide and a DLSPP waveguide was optimized by adjusting the vertical offset between them [20], [21]. The optimal loss of the end-fire coupling is about 1 dB. In the case of the hybrid structure based on photonic waveguides with the same core material as DLSPP waveguides, the DLSPP waveguides are tapered to match their dimensions to those of the photonic waveguides [22], [23]. This is because the core dimensions of the photonic waveguide are a few micrometers. When poly(methyl methacrylate) (PMMA) of refractive index 1.49 was used as a core material, the width of the loaded dielectric, w_d, was increased to the width of the core of the photonic waveguide, w_p, over a distance l_t between 25 and 35 μm [22]. The loss of the coupling via the tapering was $\sim$3 dB. When the nanoimprint lithography resist mr-NIL 6000 of refractive index 1.523 was used as a core material, the height of the loaded dielectric, h_d, as well as w_d was increased, and h_d was increased to the height of the core, h_p [23]. In this case, l_t was 50 μm, and the coupling loss was $\sim$1.8 dB. However, to our knowledge, there has been no research on an improvement of the coupling between photonic and DLSPP waveguides with the same core material. Such an improvement may pave the way for a hybrid structure with small loss, which is easily realizable since photonic and DLSPP waveguides with the same core material can be made simultaneously.

In this paper, we theoretically investigate how to improve the efficiency of the coupling between photonic and DLSPP waveguides with the same core material. The improvement means reduction of the coupling loss and the length of the tapering region, l_t, for the coupling. In Section 2, we try to do so by employing a dielectric with a refractive index higher than those of the previous loaded dielectrics. The photonic and DLSPP waveguides based on the high-index dielectric are designed, and the tapering length is optimized. In Section 3, to further reduce the coupling loss, we modify the DLSPP waveguide based on the high-index dielectric. The modified DLSPP waveguide is called a double-dielectric-loaded SPP (D^2LSPP) waveguide. We discuss the characteristics of the D^2LSPP waveguide and the coupling between the D^2LSPP waveguide and the photonic waveguide with the high-index dielectric core. Finally, concluding remarks are given in Section 4.

2. DLSPP and Photonic Waveguides Based on the Same High-Index Dielectric

The investigated photonic and DLSPP waveguides are schematically shown in Fig. 1(a) and (b), respectively. The top view of the coupling structure where the DLSPP waveguide is linearly tapered and connected to the photonic waveguide is also shown in Fig. 1(c). The two waveguides are on the same substrate. The structure's refractive index n_s was set to that of the UV-curable polymer Exguide LFR (ChemOptics Inc.) such that $n_s = 1.375$. The loaded dielectric of the DLSPP waveguide is on the gold film with thickness t_d, which was set to 0.1 μm. The refractive index of gold is $0.559 + i9.81$ at $\lambda = 1.55$ μm. It is assumed that $h_p = h_d + t_d$. In other words, we do not consider

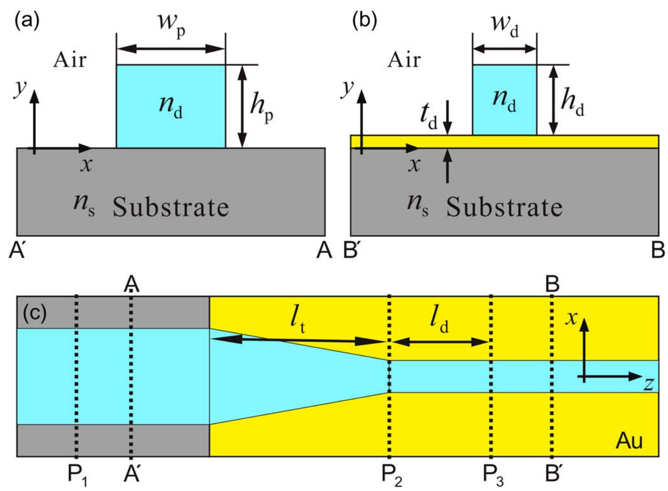

Fig. 1. (a) Cross-sectional structure of the photonic waveguide. (b) Cross-sectional structure of the DLSPP waveguide. (c) Top view of the coupling structure between the photonic waveguide and the DLSPP waveguide. It is assumed that $h_p = h_d + t_d$.

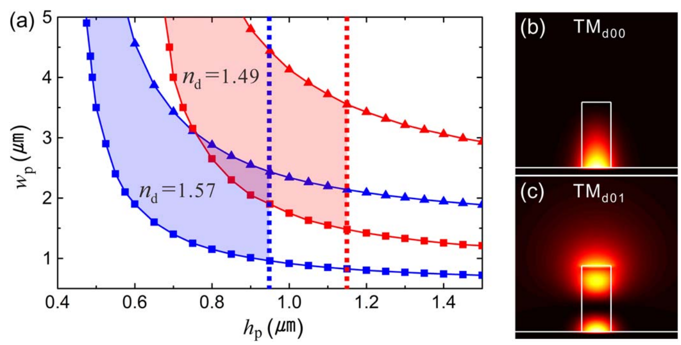

Fig. 2. (a) Region of width w_p and height h_p for which the photonic waveguide supports only the fundamental TM mode TM_{p00}. TM_{p00} is cut off if w_p and h_p are on the lower curve with square symbols. The first higher-order mode TM_{p10} is cut off if w_p and h_p are on the upper curve with triangle symbols. If h_p is on the right of the dotted line, the DLSPP waveguide supports the first higher-order mode TM_{d01}. (b) and (c) Intensity profiles of TM_{d00} and TM_{01} of the DLSPP waveguide for $h_d = 1$ μm, $w_d = 0.5$ μm, and $n_d = 1.57$.

that the DLSPP waveguide is vertically tapered since it is not easy to implement a vertically tapering structure. In the following discussion, $\lambda = 1.55$ μm.

For the efficient coupling between the photonic and DLSPP waveguides, the photonic waveguide is appropriately designed such that it supports only the fundamental mode, which is confined as tightly as possible in the core. Using the mode solver FIMMWAVE (Photon Design) based on the finite element method, we found the region of (h_p, w_p) which allows the photonic waveguide to support only the fundamental transverse-magnetic (TM) mode TM_{p00}. The two regions for $n_d = 1.49$ and 1.57 are shown in Fig. 2(a). TM_{p00} is cut off for (h_p, w_p) on the lower curve of each region. The first higher-order mode TM_{p10} is cut off for (h_p, w_p) on the upper curve of each region. (h_p, w_p) close to the upper curve of each region should be chosen to ensure that TM_{p00} is well guided. However, we cannot choose an arbitrarily large value of h_p due to two constraints. One constraint is related to fabrication of the loaded dielectric pattern. We checked that the fundamental TM mode of the DLSPP waveguide, TM_{d00}, is most tightly confined in the x direction if $w_d \cong 0.5$ μm, which is approximately equal to $\lambda/(2n_d)$. The larger the ratio of h_d to w_d is, the harder the fabrication is. If the

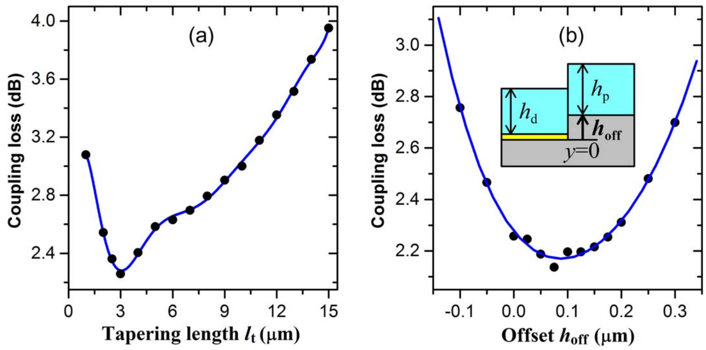

Fig. 3. (a) Relation of the coupling loss to the coupling region length l_t. (b) Relation of the coupling loss to the vertical offset h_{off} between the photonic and DLSPP waveguides. The coupling loss was calculated for $l_t = 3$ μm. The inset shows the side view of the coupling structure where the photonic waveguide is abruptly displaced at the junction. In (a) and (b), the circle symbols are obtained from the calculation based on the FDTD method. The solid lines are for illustration purposes only.

achievable ratio is 2, then h_d should be smaller than 1 μm. The other constraint is related to the single-mode operation of the DLSPP waveguide. Fig. 2(b) and (c) show the intensity distributions of TM_{d00} and the first higher-order mode TM_{d01} for $h_d = 1$ μm, $w_d = 0.5$ μm, and $n_d = 1.57$. h_d should be smaller than the specific value for which TM_{d01} is cut off. The values are 0.85 and 1.05 μm for $n_d = 1.57$ and 1.49, respectively. The values of h_p, determined from these specific values, are denoted by the vertical dotted lines in Fig. 2(a). If $n_d = 1.49$, w_p needs to be large (e.g., > 4.5 μm) for a moderate value of h_p (e.g., 0.9 μm). Then, l_t needs to be large, and the coupling loss becomes large due to metallic loss in the long tapering region. w_p can be made smaller than 3.5 μm if h_p is chosen to be close to 1.15 μm. However, in this case, it seems difficult to satisfy the first constraint. In the case of $n_d = 1.57$, the photonic waveguide with $w_p = 2.5$ μm and $h_p = 0.9$ μm supports only TM_{p00}, and TM_{p00} is far from cut-off.

The result in Fig. 2 shows that n_d needs to be large to reduce w_p and h_p such that the size mismatch between the photonic waveguide core and the loaded dielectric can be alleviated to some extent. However, if n_d is too large, it becomes inefficient to launch light into the photonic waveguide. In addition, there are few waveguide materials which have a large refractive index and can be easily processed. The negative photoresist SU-8 has a refractive index of 1.57; it can be patterned by using either optical lithography or e-beam lithography [26], [27]. In addition, it has already been used for optical waveguides [28]. Therefore, n_d was set to 1.57, and w_p, h_p, w_d, and h_d were determined to be 2.5, 0.9, 0.5, and 0.8 μm, respectively. The propagation loss α_d of the DLSPP waveguide is 0.13 dB/μm.

Using the finite-difference time domain (FDTD) method (FDTD solutions, Lumerical Inc.), the coupling structure was analyzed. TM_{p00} was launched at position P_1 in the photonic waveguide. For this input, power transmittance T was calculated at position P_3 in the DLSPP waveguide; P_3 is at a distance l_d from position P_2 where the coupling structure ends. The coupling loss of the coupling structure is defined as the subtraction of the straight DLSPP waveguide loss given by $\alpha_d \times l_d$ from $-10 \log_{10} T(\text{dB})$. The calculated coupling loss is shown as a function of l_t in Fig. 3(a). We checked that the amount of radiated fields around the tapering region decreases as l_t increases up to 3 μm. Hence, the coupling loss decreases. However, if l_t increases over 3 μm, metallic loss in the tapering region causes the coupling loss to increase. Therefore, the minimum coupling loss of 2.3 dB is obtained for $l_t = 3$ μm. The coupling loss was also calculated in a reverse way. The reverse way means that TM_{d00} was launched at P_3 and the electromagnetic fields were monitored at P_1. By applying the conjugated mode orthogonality relation to the monitored fields, the power transmittance from TM_{d00} to TM_{p00} was calculated. The coupling loss was obtained from the power transmittance, and it is 2.2 dB for $l_t = 3$ μm. Consequently, when $l_t = 3$ μm, TM_{p00} most efficiently excites TM_{d00}, and vice versa. This value of l_t is about one tenth of the previous values in [22], [23], and the coupling loss is smaller than that in [22].

The influence of the vertical offset between the two waveguides on the coupling loss was also analyzed. As shown in the inset of Fig. 3(b), the core of the photonic waveguide is displaced upwards (downwards) if the displacement $h_{\rm off}$ is positive (negative). For simplicity, we assumed that an abrupt junction exists between the two waveguides. The coupling loss calculated for $l_t = 3\ \mu$m, $h_d = 0.8\ \mu$m, and $h_p = 0.8\ \mu$m is shown in Fig. 3(b) with respect to the displacement $h_{\rm off}$. As $h_{\rm off}$ increases, the fields of TM_{p00} in the substrate are more efficiently coupled to the DLSPP waveguide. However, if $h_{\rm off}$ keeps increasing, the fields of TM_{p00} in the region for $y > h_d + t_d$ are not coupled to the DLSPP waveguide since TM_{d00} is well confined in the loaded dielectric of height h_d. Therefore, when $h_{\rm off} = 75$ nm, the coupling loss is minimized at 2.1 dB. As explained in Introduction, the vertical offset between a silicon photonic waveguide and a DLSPP waveguide is appropriately determined such that the loss of the end-fire coupling is minimized. However, in the case of the hybrid structure consisting of the SU-8-based photonic and DLSPP waveguides, the vertical offset has no clear advantage in reducing the coupling loss. A different method is required to further reduce the coupling loss.

3. D^{2}LSPP Waveguide

The coupling loss is mainly caused by the fact that TM_{d00} does not have fields below $y = 0\ \mu$m but TM_{p00} does. Therefore, the fields of TM_{p00} below $y = 0$ should be reduced to further decrease the coupling loss. This can be achieved by increasing h_p. However, the increase of h_p results in an increase of h_d such that TM_{d01} is supported by the DLSPP waveguide. To solve this problem, we modify the DLSPP waveguide into the D^{2}LSPP waveguide shown in Fig. 4(a). The second dielectric of refractive index n_{d2} and height h_{d2} is placed in between the gold film and the loaded dielectric. $n_{d2} < n_d$, and $h_p = h_d + h_{d2} + t_d$. The D^{2}LSPP waveguide is similar to a silicon-based hybrid plasmonic waveguide with a metal cap [29]. However, the D^{2}LSPP waveguide is not a hybrid plasmonic waveguide since the difference between n_d and n_{d2} is small enough that light is not strongly confined in the second dielectric. The intensity distribution of the fundamental TM mode, which is still denoted by TM_{d00}, of the D^{2}LSPP waveguide is shown in Fig. 4(b) for $h_d = 0.6\ \mu$m, $n_{d2} = 1.45$, and $h_{d2} = 0.4\ \mu$m. It is similar to that of the DLSPP waveguide. Because of the second dielectric, we can increase h_p to some extent while maintaining the single-mode operation of the D^{2}LSPP waveguide. In addition, the fields of TM_{d00} shift upwards [see Fig. 4(e)]. Consequently, TM_{p00} better matches TM_{d00} of the D^{2}LSPP waveguide than TM_{d00} of the DLSPP waveguide.

The refractive index of the second dielectric, n_{d2}, was set to 1.45. There are a few materials with this refractive index. For example, the negative e-beam resist hydrogen silsesquioxane (HSQ) may be used. HSQ has been also used for optical waveguides [30]. We expect that it would be possible to simultaneously pattern SU-8 and HSQ by using e-beam lithography. In addition, the UV-curable polymer Exguide ZPU13 (ChemOptics Inc.) can be used. In this case, SU-8 is first patterned by using optical lithography, and the second dielectric is dry-etched by using the SU-8 pattern as an etching mask.

We checked that the D^{2}LSPP waveguide supports only TM_{d00} when $h_d + h_{d2} \le 1\ \mu$m and $h_{d2} \ge 0.2\ \mu$m. With h_d and h_{d2} varied under the constraint that $h_d + h_{d2} = 1\ \mu$m and $h_{d2} \ge 0.2\ \mu$m, the effective mode area and propagation loss of TM_{d00} were calculated. The effective mode area is defined as $[\int W(\mathbf{r}dA)]^2/[\int W(\mathbf{r})^2 dA]$, where $W(\mathbf{r})$ is the energy density [31]. The calculated effective mode area and propagation loss are shown in Fig. 4(c) with respect to h_{d2}. As h_{d2} increases, the fields of TM_{d00} become weak on the gold surface, and they are more widely distributed in the loaded double dielectrics. This can be confirmed from the distributions of the magnitude of the y-component of the electric field of TM_{d00}, $|E_y|$, along the vertical centerline of the loaded double dielectrics; they are shown in Fig. 4(d) and (e) for $h_{d2} = 0.2$ and $0.4\ \mu$m, respectively. Hence, the effective mode area increases, and the propagation loss decreases. However, if h_{d2} increases further, the fields become strong on the gold surface again as shown in the distribution of $|E_y|$ for $h_{d2} = 0.8\ \mu$m in Fig. 4(f). In other words, the D^{2}LSPP waveguide behaves like a DLSPP waveguide. Therefore, the effective mode area decreases, and the propagation loss increases.

The D^{2}LSPP waveguide is connected to the photonic waveguide in the same way as the DLSPP waveguide: the top view of the coupling structure for the D^{2}LSPP waveguide is the same as shown in

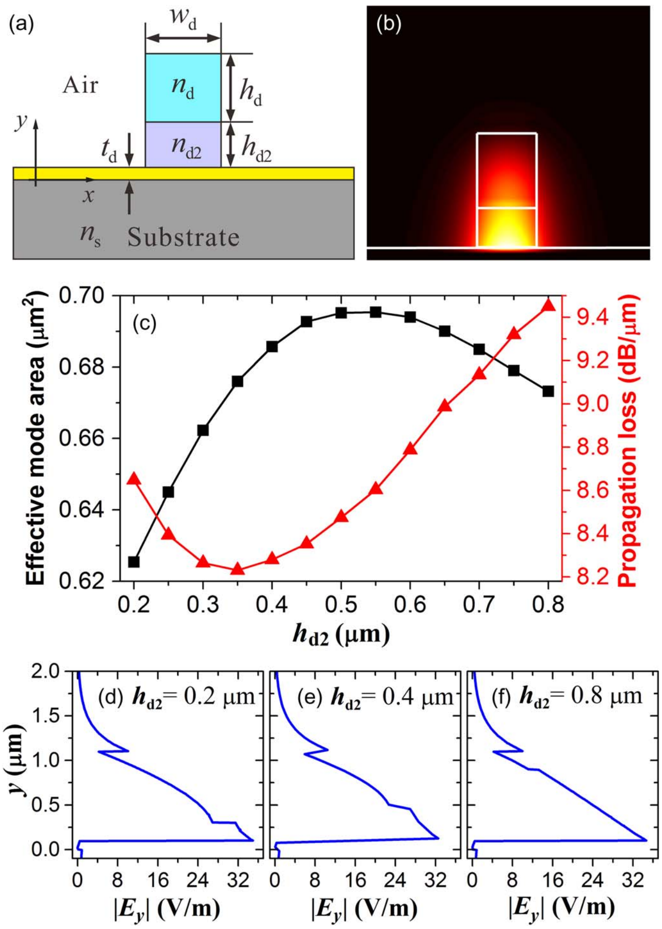

Fig. 4. (a) Cross-sectional structure of the D^{2}LSPP waveguide. (b) Intensity profile of the fundamental TM mode TM_{d00} of the D^{2}LSPP waveguide for $h_d = 0.6$ μm, $h_{d2} = 0.4$ μm, and $n_{d2} = 1.45$. (c) Relations of the effective mode area and propagation loss of TM_{d00} to h_{d2}. (d), (e), and (f) show the distributions of the magnitude of the y-component of the electric field of TM_{d00}, $|E_y|$, along the vertical centerline of the loaded dielectric for $h_{d2} = 0.2$, 0.4 and 0.8 μm, respectively.

Fig. 1(c). For some values of h_d and h_{d2}, we calculated the coupling loss as a function of l_t, and the calculation results are shown in Fig. 5(a). Similar to the result in Fig. 3(a), as l_t increases, the loss due to the radiated fields in the tapering region decreases, and the metallic loss increases. Hence, the coupling loss is minimized when $l_t = 4$ μm. Next, the coupling loss was calculated as a function of h_{d2} while l_t was set to 4 μm. The calculation result is shown in Fig. 5(b). As the effective mode area of TM_{d00} increases and the propagation loss in the tapering region decreases, the coupling loss decreases. For h_{d2} near 0.4 μm, the effective mode area is maximized, and the propagation loss is minimized, as shown in Fig. 4(c). When $h_d = 0.6$ μm and $h_{d2} = 0.4$ μm, the coupling loss is minimum, being equal to 1.1 dB. Consequently, the use of the D^{2}LSPP waveguide with $h_d = 0.6$ μm and $h_{d2} = 0.4$ μm enables the coupling loss to be reduced from 2.3 dB to 1.1 dB and the propagation loss α_d to be reduced from 0.13 dB$/\mu$m to 0.083 dB$/\mu$m. However, l_t increases from 3 μm to 4 μm, and the effective mode area increases from 0.5 μm^2 to 0.68 μm^2.

4. Conclusion

In summary, we have investigated how to improve the efficiency of the coupling between photonic and DLSPP waveguides with the same core material. We have developed methods of reducing the

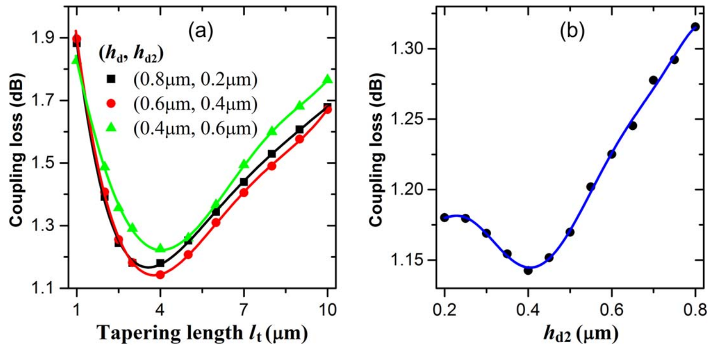

Fig. 5. (a) Relations of the coupling loss to l_t for some values of h_d and h_{d2}. (b) Relation of the coupling loss to h_{d2} for $l_t = 4$ μm. The symbols are obtained from the calculation based on the FDTD method. The solid lines are for illustration purposes only.

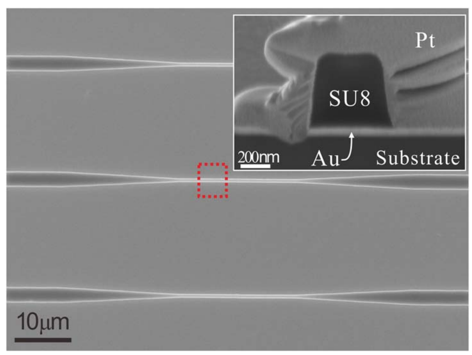

Fig. 6. Surface SEM image of an SU-8 pattern formed on a gold film. The inset shows an enlarged image of the cross-section of the SU-8 pattern in the box. The SU-8 pattern was covered by Pt in order to form the cross-section by using focused ion beam milling.

coupling loss and the tapering length. First, the lithographically patternable SU-8, which has a larger refractive index than the dielectrics of the previous DLSPP waveguides, is employed as a core material. Then, the photonic and DLSPP waveguides are designed to support only the well-confined fundamental mode. The photonic waveguide can be coupled to the DLSPP waveguide with a minimum coupling loss of 2.3 dB through a 3-μm-long tapering region. The coupling loss and the tapering region length are smaller than those reported previously. The coupling loss is further reduced by modifying the DLSPP waveguide into a D^2LSPP waveguide. In the D^2LSPP waveguide, SU-8 and another dielectric of refractive index 1.45 (e.g., HSQ) are loaded on the gold film. When the thicknesses of the second dielectric and SU-8 are 0.4 and 0.6 μm, respectively, the photonic waveguide can be coupled to the D^2LSPP waveguide with a minimum coupling loss of 1.1 dB through a 4-μm-long coupling region.

A hybrid structure consisting of the photonic waveguides and the DLSPP or D^2LSPP waveguides studied in this work is expected to be useful for an easily-realizable hybrid planar lightwave circuit with relatively low loss. A light source or a photodetector is connected to such a hybrid structure through a small-core fiber. If a small-core fiber of core diameter 1.8 μm and numerical aperture 0.35 (UHNA3, Nufern Inc.) is used, the loss of the butt-coupling between the fiber and the photonic waveguide is 3.1 dB. This is similar to the loss of the coupling between a single-mode fiber and the photonic waveguide in [22]. A preliminary experiment for realization of such a hybrid structure is to make a submicron SU-8 pattern with an aspect ratio larger than 1 on a gold film. Although the adhesion of SU-8 to gold is poor, a SU-8 pattern can be well formed on a gold film by using the adhesion promoter ZAP1020 (ChemOptics Inc.). A surface scanning electron microscope (SEM) image and a cross-sectional SEM image of the SU-8 pattern are shown in Fig. 6. The width and height of the pattern are 0.5 and 0.8 μm, respectively. Based on this result, the hybrid structure may be developed soon.

References

[1] H. Raether, *Surface Plasmons on Smooth and Rough Surfaces and on Grating,* 1st ed. Berlin, Germany: Springer-Verlag, 1988.

[2] E. Ozbay, "Plasmonics: Merging photonics and electronics at nanoscale dimensions," *Science*, vol. 311, no. 5758, pp. 189–193, Jan. 2006.

[3] Z. Han, A. Y. Elezzabi, and V. Van, "Experimental realization of subwavelength plasmonic slot waveguides on a silicon platform," *Opt. Lett.*, vol. 35, no. 4, pp. 502–504, Feb. 2010.

[4] R. Salas-Montiel *et al.,* "Quantitative analysis and near-field observation of strong coupling between plasmonic nanogap and silicon waveguides," *Appl. Phys. Lett.*, vol. 100, no. 23, pp. 231109-1–231109-4, Jun. 2012.

[5] H. Choo *et al.,* "Nanofocusing in a metal-insulator-metal gap plasmon waveguide with a three-dimensional linear taper," *Nat. Photon.*, vol. 6, no. 12, pp. 838–844, Dec. 2012.

[6] M.-S. Kwon, "Metal-insulator-silicon-insulator-metal waveguides compatible with standard CMOS technology," *Opt. Exp.*, vol. 19, no. 9, pp. 8379–8393, Apr. 2011.

[7] S. Zhu, G. Q. Lo, and D. L. Kwong, "Components for silicon plasmonic nanocircuits based on horizontal Cu–SiO_2–Si–SiO_2–Cu nanoplasmonic waveguides," *Opt. Exp.*, vol. 20, no. 6, pp. 5867–5881, Mar. 2012.

[8] M.-S. Kwon, J.-S. Shin, S.-Y. Shin, and W.-G. Lee, "Characterization of realized metal-insulator-silicon-insulator-metal waveguides and nanochannel fabrication via insulator removal," *Opt. Exp.*, vol. 20, no. 20, pp. 21 875–21 887, Sep. 2012.

[9] J.-S. Shin, M.-S. Kwon, C.-H. Lee, and S.-Y. Shin, "Investigation and improvement of 90° direct bends of metal-insulator-silicon-insulator-metal waveguides," *IEEE Photon. J.*, vol. 5, no. 5, p. 6601909, Oct. 2013.

[10] M. P. Nielsen, A. Ashfar, K. Cadien, and A. Y. Elezzabi, "Plasmonic materials for metal-insulator-semiconductor-insulator-metal nanoplasmonic waveguides on silicon-on-insulator platform," *Opt. Mater.*, vol. 36, no. 2, pp. 294–298, Dec. 2013.

[11] C. Reinhardt *et al.,* "Laser-fabricated dielectric optical components for surface plasmon polaritons," *Opt. Lett.*, vol. 31, no. 9, pp. 1307–1309, May 2006.

[12] B. Steinberger *et al.,* "Dielectric stripes on gold as surface plasmon waveguides," *Appl. Phys. Lett.*, vol. 88, no. 9, pp. 094104-1–094104-3, Feb. 2006.

[13] T. Holmgaard and S. I. Bozhevolnyi, "Theoretical analysis of dielectric-loaded surface plasmon-polariton waveguides," *Phys. Rev. B, Condens. Matter*, vol. 75, no. 24, pp. 245405-1–245405-12, Jun. 2007.

[14] S. Randhawa *et al.,* "Performance of electro-optical plasmonic ring resonators at telecom wavelengths," *Opt. Exp.*, vol. 20, no. 3, pp. 2354–2362, Jan. 2012.

[15] C. Garcia, V. Coello, Z. Han, I. P. Radko, and S. I. Bozhevolnyi, "Partial loss compensation in dielectric-loaded plasmonic waveguides at near infra-red wavelengths," *Opt. Exp.*, vol. 20, no. 7, pp. 7771–7776, Mar. 2012.

[16] Z. Zhu, C. E. G. Ortiz, Z. Han, I. P. Radko, and S. I. Bozhevolnyi, "Compact and broadband directional coupling and demultiplexing in dielectric-loaded surface plasmon polariton waveguides based on the multimode interference effect," *Appl. Phys. Lett.*, vol. 103, no. 6, pp. 061108-1–061108-5, Aug. 2013.

[17] O. Tsilipakos, T. V. Yioultsis, and E. E. Kriezis, "Theoretical analysis of thermally tunable microring resonator filters made of dielectric-loaded plasmonic waveguides," *J. Appl. Phys.*, vol. 106, no. 9, pp. 093109-1–093109-8, Nov. 2009.

[18] J. Gosciniak *et al.,* "Thermo-optic control of dielectric-loaded plasmonic waveguide components," *Opt. Exp.*, vol. 18, no. 2, pp. 1207–1216, Jan. 2010.

[19] J. Gosciniak, L. Markey, A. Dereux, and S. I. Bozhevolnyi, "Efficient thermo-optically controlled Mach-Zhender interferometers using dielectric-loaded plasmonic waveguides," *Opt. Exp.*, vol. 20, no. 15, pp. 16 300–16 309, Jul. 2012.

[20] R. M. Briggs, J. Grandidier, S. P. Burgos, E. Feigenbaum, and H. A. Atwater, "Efficient coupling between dielectric-loaded plasmonic and silicon photonic waveguides," *Nano Lett.*, vol. 10, no. 12, pp. 4851–4857, Dec. 2010.

[21] O. Tsilipakos *et al.,* "Interfacing dielectric-loaded plasmonic and silicon photonic waveguides: Theoretical analysis and experimental demonstration," *IEEE J. Quantum Electron.*, vol. 48, no. 5, pp. 678–687, May 2012.

[22] J. Gosciniak *et al.,* "Fiber-coupled dielectric-loaded plasmonic waveguides," *Opt. Exp.*, vol. 18, no. 5, pp. 5314–5319, Mar. 2010.

[23] A. Seidel *et al.* (2010). Fiber-coupled surface plasmon polariton excitation in imprinted dielectric-loaded waveguides. *Int. J. Opt.* [Online]. 2010, pp. 897829-1–897829-6. Available: http://dx.doi.org/10.1155/2010/897829

[24] Q. Li, Y. Song, G. Zhou, Y. Su, and M. Qiu, "Asymmetric plasmonic-dielectric coupler with short coupling length, high extinction ratio, low insertion loss," *Opt. Lett.*, vol. 35, no. 19, pp. 3153–3155, Oct. 2010.

[25] L. Chen, X. Li, and D. Gao, "An efficient directional coupling from dielectric waveguide to hybrid long-range plasmonic waveguide on a silicon platform," *Appl. Phys. B*, vol. 111, no. 1, pp. 15–19, Apr. 2013.

[26] V. Kudryashov, X.-C. Yuan, W.-C. Cheong, and K. Radhakrishnan, "Grey scale structures formation in SU-8 with e-beam and UV," *Microelectron. Eng.*, vol. 67/68, pp. 306–311, Jun. 2003.

[27] A. Campo and C. Greiner, "SU-8: A photoresist for high-aspect-ratio and 3D submicron lithography," *J. Micromech. Microeng.*, vol. 17, no. 6, pp. R81–R95, Jun. 2007.

[28] B. Bêche, N. Pelletier, E. Gavot, and J. Zyss, "Single-mode TE_{00}–TM_{00} optical waveguides on SU-8 polymer," *Opt. Commun.*, vol. 230, no. 1–3, pp. 91–94, Jan. 2004.

[29] Y. Song, J. Wang, Q. Li, M. Yan, and M. Qiu, "Broadband coupler between silicon waveguide and hybrid plasmonic waveguide," *Opt. Exp.*, vol. 18, no. 12, pp. 13 173–13 179, Jun. 2010.
[30] M. P. Nezhad, O. Bondarenko, M. Khajavikhan, A. Simic, and Y. Fainman, "Etch-free low loss silicon waveguides using hydrogen silsesquioxane oxidation masks," *Opt. Exp.*, vol. 19, no. 20, pp. 18 827–18 832, Sep. 2011.
[31] R. F. Oulton, G. Bartal, D. F. P. Pile, and X. Zhang, "Confinement and propagation characteristics of subwavelength plasmonic modes," *New J. Phys.*, vol. 10, no. 10, pp. 105018-1–105018-14, Oct. 2008.